ORIGINAL ARTICLE

Effect of technological voids on hydro-mechanical behavior of compacted bentonite

Yunzhi Tan[1,2] · Shixiang Hu[1,2] · Hui Li[1,2] · Huajun Ming[2] · Jun Wu[1,2]

Abstract

In the high-level radioactive waste geological disposal, the gaps between the waste canisters, buffer layer, and surrounding rock, will affect the hydro-mechanical behavior of bentonite blocks. In this paper, the gaps between the buffer layers were simulated by setting different technological void widths. The interaction between technological void width and the swelling pressure and hydraulic conductivity of compacted bentonite was investigated. Meanwhile, the effect of different boundary conditions on the hydration process of compacted bentonite simulated through stepwise pre-set technological void (SV) and completely pre-set technological void (CV) was studied. The results showed that, keeping the same dry density, the swelling pressure of compacted bentonite blocks with 33% technological voids remained unchanged compared to specimens without voids, while the hydraulic conductivity increased by 10%. Comparing the SV with CV specimens, the swelling pressure was similar, but the hydraulic conductivity of the latter increased by 6%. Microstructural test results indicated differences in overall homogeneity between compacted bentonite blocks with 33% technological voids and those without voids after complete hydration, and distinct differences were also observed between the void and block areas in specimens with voids. The SV method reduced the cumulative pore volume in the void area, resulting in a more uniform hydration process.

Keywords Compacted bentonite · Technological voids · Boundary conditions · Swelling pressure · Hydraulic conductivity · Microstructure

Introduction

With the widespread use of nuclear energy, an amount of high-level radioactive waste (HLW) is generated, posing a serious threat to human living environment if not safely disposed. Currently, deep geological disposal is recognized worldwide as the most feasible method to isolate high-level waste from the biosphere for at least tens of thousands of years (Birkholzer et al. 2012). It consists of waste canisters, buffer/backfill layers, and host rock. Eventually, a multi-barrier system is formed to prevent the migration of radioactive nuclides to the external environment. Among them,

the buffer layer is required to provide core functions of isolation, pollutant adsorption, and deformation buffering against the surrounding rock (ENRESA 2000; Posiva SKB 2017). Highly compacted bentonite, is considered as the most ideal material for buffer/backfill in high-level waste disposal facilities, due to low permeability, strong adsorption, and suitable swelling pressure, filling the space between waste canisters and the surrounding rock (Komine 2020; Villar et al. 2021a, b; Tan et al. 2021).

However, during the assembly of compacted bentonite blocks, various construction technological voids inevitably exist in the multi-barrier system of geological disposal such as between the blocks, between the blocks and the waste canisters, and between the blocks and the surrounding rock (Gunnarsson 2006; Martikainen et al. 2018; Dueck et al. 2011; Feng et al. 2024). According to statistics, the volume of construction technological voids accounts for 6.6–14% of the total volume of disposal facility galleries (Martín et al. 2006; Wang et al. 2021a, b). In fact, these technical voids are difficult to deal with, mainly relying on the self-sealing

✉ Hui Li
201708140021008@ctgu.edu.cn

1 Key Laboratory of Geological Hazards on Three Gorges Reservoir Area, Ministry of Education, China Three Gorges University, Yichang 443002, China

2 Yichang Key Laboratory of the Resources Utilization for Problematic Soils, China Three Gorges University, Yichang 443002, China

ability of compacted bentonite or filling with granular bentonite to complete the seal (Liu et al. 2021).

Some studies indicate that neglecting the treatment of voids may impact the safety of disposal repositories. Villar et al. (2005) discovered that technological voids created preferential pathways for water flow, although these pathways would gradually close as FEBEX bentonite hydrated. Mokni et al. (2016) identified that the existence of technological voids introduced new sources of hydration (annular voids) and flow paths (voids between blocks) that altered saturation kinetics. Chen et al. (2016) reported that hydraulic fracturing occurs when groundwater pressure exceeds the hydraulic resistance of the interfaces, and the presence of technological gaps increases the risk of hydraulic fracturing. Harrington et al. (2020) highlighted that the uneven development of pore-water pressure and its interaction with total stress within the bentonite might hinder homogenization during the self-sealing process, potentially affecting hydraulic-mechanical performance and even posing risks to disposal safety. Some researchers have focused on the study of void volume considering the non-strict confinement brought by voids, and quantifying the impact of voids on disposal repositories. Wang et al. (2013) contended that technological voids had no impact on the final swelling pressure, which can be determined through a unique relationship between swelling pressure and bentonite void ratio. However, Jia et al. (2019) discovered that the axial final swelling pressure tended to decrease when the axial void volume exceeded 14.3% of the final volume (16.7% of the initial sample volume). For compacted bentonite blocks, the adverse effects brought by voids on macroscopic hydraulic-mechanical performance stem from the inherent non-uniformity of the overall structure during the self-sealing process. Gens et al. (2011) emphasized that the uneven distribution of buffer material significantly impacted the local hydraulic and mechanical properties of compacted bentonite, consequently influencing the engineered barrier's performance. Bian et al. (2019) revealed that voids in the compacted bentonite blocks divided them into swelling and compression zones. Changes in dry density and water content were used to interpret the heterogeneous distribution in terms of microstructure along the sample and its variation with time. Jia et al. (2019) conducted MIP tests to explore the impact of gaps on the inhomogeneity and microstructure distribution of bentonite. It can be observed that the uniformity of pore structure is one of the crucial indicators to evaluate compacted bentonite blocks. Therefore, further experimental research is necessary to study the non-uniform microstructural distribution of bentonite.

There are also many studies on filling technological voids with pellet bentonite (García et al. 2015; Narea 2019; Wang et al. 2021a, b; Villar et al. 2021a, b; Gens et al. 2021). In general, the method for filling pellets can ameliorate the adverse effects of technological voids on the buffer barrier function and enhance overall impermeability. When the voids are filled, the boundary conditions of the compacted bentonite specimen change from free swelling to restricted swelling, leading to a change in the stress release pathway of the bentonite blocks. However, the existing research mainly focuses on the overall performance of the voids after filling, and there are fewer studies on the development of restricted swelling of the bentonite blocks in the system. Therefore, a series of swelling pressure and hydraulic conductivity tests, under constant-volume conditions were conducted in this study to investigate the effect of technological void width on compacted bentonite. Furthermore, different boundary conditions were simulated by the methods of stepwise pre-set-technological void (SV) and complete pre-set-technological void (CV), SV representing the voids filled with pellets and the block expansion process was hindered, and CV representing the voids unfilled with pellets. The effect of boundary conditions on the hydration process of compacted bentonite after assuming filled pellets was finally investigated.

Testing materials and specimen preparation

Materials

The bentonite was sourced from Gongyi, Henan Province, with a montmorillonite content of 82.3%. According to "Standard for Geotechnical Testing" (GB/T50123-1999), the density, liquid limit, and free swelling ratio of the bentonite were measured. The physicochemical properties and major chemical composition are presented in Table 1. X-ray fluorescence (XRF) results revealed that the bentonite is rich in silicon and aluminum oxides, accounting for 87.1% of the total content, followed by small amounts of sodium, iron, potassium, and magnesium oxides. It can be described as sodium bentonite (Na-bentonite).

Specimen preparation

Before specimen preparation, the bentonite powder was stored in a sealed chamber containing saturated K_2CO_3 solution. After about 1 month, the suction equilibrium was reached, the water content in mass was 11%. According to the initial water content, target dry density, and ring dimensions (inner diameter 50 mm, height 10 mm; inner diameter 50 mm, height 15 mm), the mass of bentonite powder was calculated and poured into the mold. Then, the bentonite powder was compacted into a cutting ring mold by a press machine. During the uniaxial compaction stage, the loading rate was controlled at 0.5 mm/min until reaching the target density, the maximum pressure was maintained for 2 h to minimize the vertical rebound of the specimen.

Table 1 Basic properties of bentonite powder

Property	Description	
Specific gravity	2.76	
Liquid limit (%)	273.6	
Plastic limit (%)	37.5	
Specific surface area (m^2/g)	634.8	
Free swelling ratio (%)	360	
Cation Exchange Capacity (meq/100 g)	68	
Mineral component (%)	Montmorillonite	82.3
	Illite	5.4
	Calcite	1.2
	Cristobalite	7.6
	Quartz	1.4
	Others	2.1
Main chemical composition (%)	Al_2O_3	15.3
	SiO_2	71.8
	Fe_2O_3	4.5
	Na_2O	3.4
	MgO	1.8
	K_2O	1.2
	Other	2

Subsequently, the press machine was raised, the specimens' preparation was completed. After recheck, both the height and diameter of the sample meet the pre-designed requirements.

Methods

Testing plan

The testing plan is shown in Tables 2 and 3. After the cylindrical rings with specimens were placed into the testing setups (Fig. 1), a pre-set space was created by adjusting the dial gauge and positioning screw to fix the piston height to simulate axial voids. Tests A1–A5 were the completely pre-set technological void, in detail, at the beginning of the tests, the piston was moved upward to create a predetermined height of void in the upper part of the specimen, then the swelling pressure and saturated hydraulic tests were conducted. Test A6 was the stepwise pre-set technological void, that was, the specimen was installed without technological void, and the hydration test was performed until the specimen is completely saturated and the swelling pressure

Table 2 Initial and final conditions for specimens

Testing type	Specimen No.	Compacted dry density (g/cm^3)	Initial height (mm)	Void thickness (mm)	Swelling volume ratio (%)	Final dry density (g/cm^3)
Not void	N1	1.100	15	0	0	1.100
	N2	1.650	10	0	0	1.650
Axial void	A1	1.650	10	1	10	1.50
	A2	1.650	10	2	20	1.375
	A3	1.650	10	3	30	1.269
	A4	1.650	10	4	40	1.179
	A5	1.650	10	5	50	1.100
	A6	1.650	10	0, 2, 4, 5	50	1.100

Table 3 Testing plan

Testing No.	Testing purpose	Testing content
N2, A1–A5	To investigate the hydro-mechanical behaviors under different void widths	Swelling pressure and hydraulic conductivity tests
N1, A5	To investigate the effect of the bentonite with or without voids on hydro-mechanical behaviors	Swelling pressure, hydraulic conductivity tests Water content, MIP, SEM tests for saturated specimens
A5, A6	To investigate the effect of different boundary conditions on hydro-mechanical behaviors of bentonite	Swelling pressure, hydraulic conductivity tests Water content, MIP, SEM tests for saturated specimens

A1–A5 were the completely pre-set technological void tests, the void widths are 1, 2, 3, 4 and 5 mm; N1 was the control group with no per-set technological voids, the void width is 0 mm; A6 was the stepwise pre-set technological void test, the void width changes from 0 to 2 to 4 to 5 mm
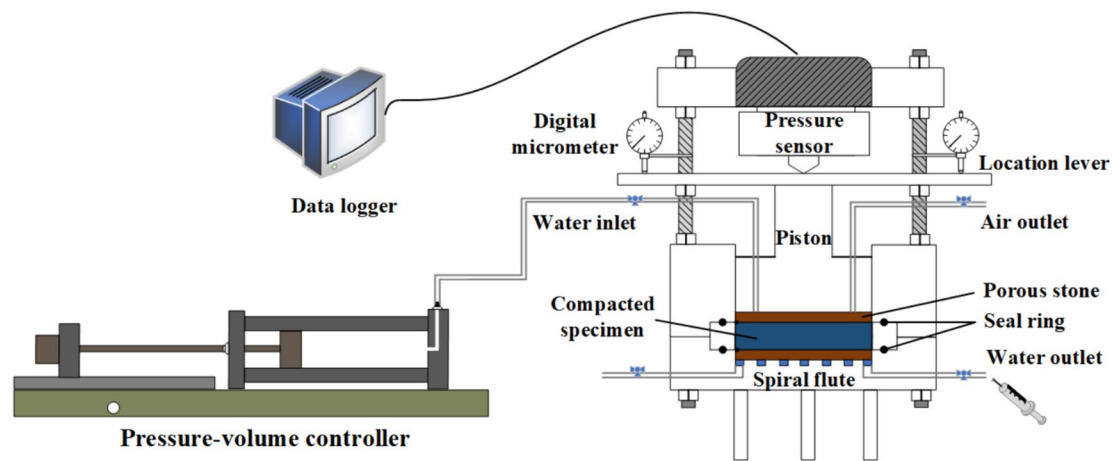
Fig. 1 Testing setups for measuring swelling pressure and saturated hydraulic conductivity

stabilizes. Then, the piston was raised to create a 2 mm void space, and the hydration test was repeated. The process was repeated again after saturation, and the movement of the piston followed the pathway with 0–2–4–5 mm. Compared with tests A5 and A6, the development modes of bentonite under different boundary conditions were obtained. N1 was the control group with no per-set technological voids (NV) to investigate whether the technological void has effect on bentonite under the same final dry density. The testing processes for N1, A5, and A6 were illustrated in Fig. 2. The swelling volume ratio of the specimens was calculated using the following formula:

$$S = \frac{\Delta V}{V_i} \times 100 \tag{1}$$

where S is the swelling volume ratio, ΔV is the void volume, and V_i is the initial volume.

Swelling pressure and hydraulic conductivity tests

After the specimens were installed, deionized water was injected from the upper water inlet above the testing setups using a pressure–volume controller (water injection pressure: 10 kPa), air was exhausted from the bottom spiral flute to ensure the accuracy of the tests. Once the air was removed, the water injection pressure was increased to 50 kPa to start the swelling pressure tests (Zeng et al. 2020). When the specimen started swelling and contacted the piston, the force was transmitted to the pressure sensor, and the swelling force was displayed in the data collector. The swelling pressure test was considered completed when the pressure sensor reading reached stabilization, remained unchanged for 48 h. The allowable deformation of the specimen was less than 10^{-4} mm during the entire test process (Zhang et al.

2018). It should be noted that during the swelling process, the bentonite generates friction with the interior of the testing setups. However, this friction force is extremely small compared to the overall swelling pressure, which can be considered negligible in this context (Harrington et al. 2020).

After the swelling pressure test, the water injection pressure was increased to 300 kPa to accelerate the overall permeation process. When water was observed to seep out, the mass of the seepage water was weighed and recorded once a day. Then, assuming uniform specimen permeability, the hydraulic conductivity coefficient was calculated according to Darcy's law, as presented in the following formula:
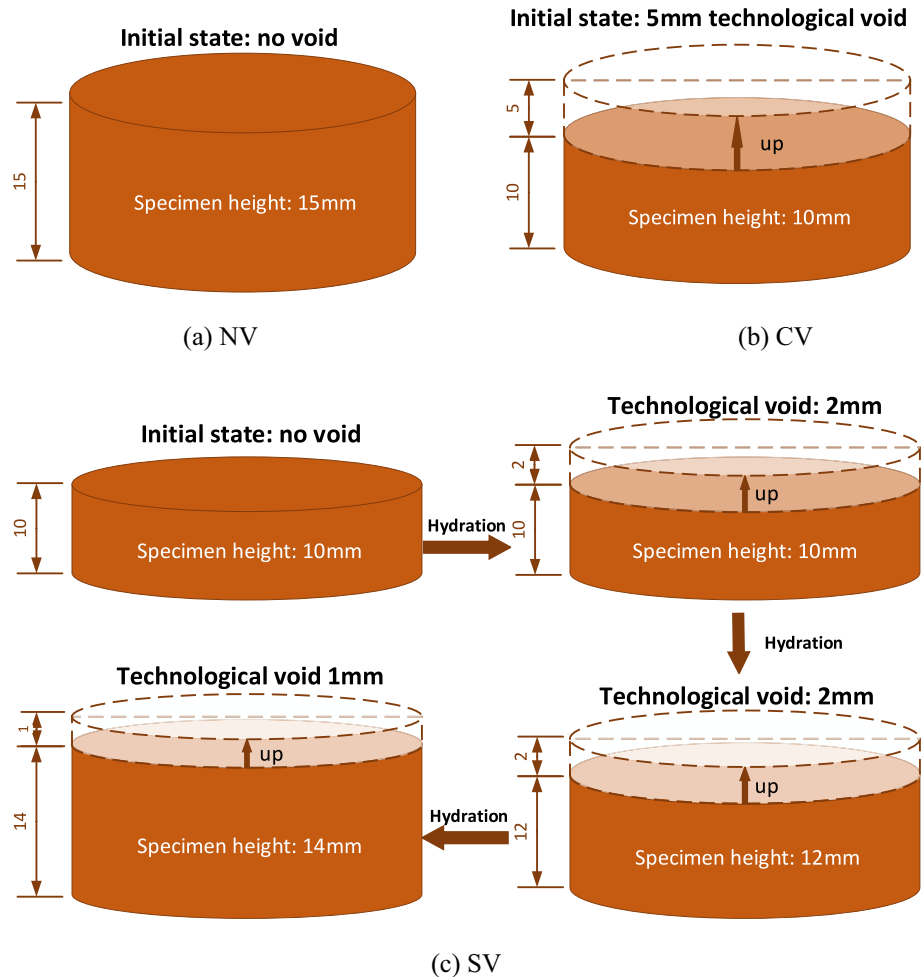
$$k = \frac{QL}{A\Delta ht} \tag{2}$$

where k is the hydraulic conductivity (m/s), Q is the mass of water/solution seepage (g), L is the flow length (m), A is the cross-sectional area (m^2), Δh is the water level difference (m), and t is the time interval (s).

Microstructural tests

The upper (void) layer, middle layer, and lower layer of saturated specimens (N1, A5, and A6) were separately taken and placed in an oven at 105 °C until a constant weight was achieved for water content determination. Cubic blocks were cut from the upper void layer and the lower layer of the void specimens, and the specimens were pre-treated using liquid nitrogen freeze-drying. Then, Scanning Electron Microscope (SEM) tests were conducted to observe morphological characteristics and pore sizes. Mercury Intrusion Porosimetry (MIP) experiments were carried out to investigate the distribution pattern of pores.

Fig. 2 Schematic diagram of the testing procedures

Initial state: no void

15

Specimen height: 15mm

(a) NV

Initial state: 5mm technological void

5

10

up

Specimen height: 10mm

(b) CV

Initial state: no void

10

Specimen height: 10mm

→ Hydration →

Technological void: 2mm

2

10

up

Specimen height: 10mm

↓ Hydration

Technological void 1mm

1

14

up

Specimen height: 14mm

← Hydration ←

Technological void: 2mm

2

12

up

Specimen height: 12mm

(c) SV

Testing results and discussions

Swelling pressure and saturated hydraulic conductivity

The development curves of the swelling pressure for specimens with different pre-set technological void widths (N1, A1–A5) are shown in Fig. 3. After deionized water infiltrated, the voids were firstly filled, and then the bottom bentonite specimen expanded, gradually filling the voids. Subsequently, the specimen underwent hydration saturation under constant volume conditions. The presence of voids changes the saturation kinetics mechanism during the swelling process of bentonite blocks. In the initial state, the bentonite block swells directly to the void area. When the void area is filled by the bentonite, its dry density is still low, leading to a low swelling pressure, and the bentonite blocks at the bottom continue to extrude towards the void area. The bentonite in the block part was the first to participate in the sealing process of the voids, leading to a delayed and reduced development of itself axial expansion stress in the block part. This phenomenon is known as "stress compensation" (Bian et al.
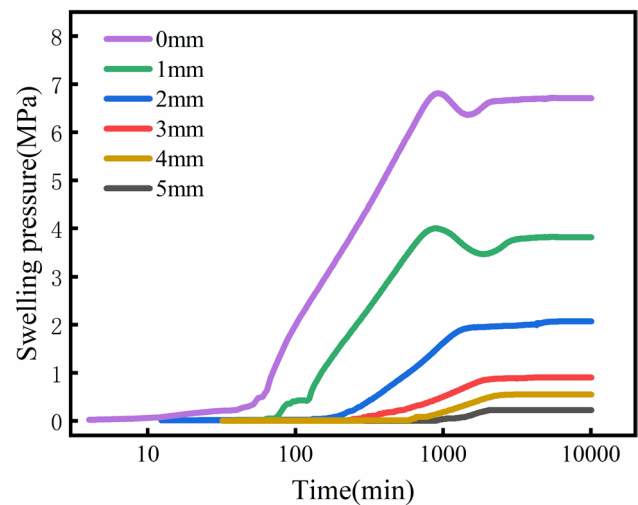
Fig. 3 Swelling pressure development under different void widths

2019). The larger the void volume in the block, the more axial stress compensation occurs, leading to lower swelling pressure and the development rate of swelling pressure.

Correspondingly, the turning point of swelling pressure stress was shifted.

It was worth noting that for specimens with technological void widths of 0 mm and 1 mm, the swelling volume was relatively small, and the compactness was high, showing a phenomenon of "stress collapse" (Zhu et al. 2013). In detail, the first peak in the hydration process is caused by the expansion of crystal layers, while the second peak is caused by the double-layer diffusion.

The swelling pressure and hydraulic conductivity for specimens with different technological void widths are shown in Fig. 4. As the void width increased, the swelling pressure decreased and the hydraulic conductivity increased. Overall, the void width exhibited an exponential development pattern with the swelling pressure and a linear pattern with the hydraulic conductivity. It can be explained that the soil becomes loose after void filling, the swelling potential was weakened, thus increasing the saturated hydraulic conductivity (Chen et al. 2012). The swelling pressure and hydraulic conductivity for specimens with different average dry density are shown in Fig. 5, the fitting curve of the average dry density relation is the same as that of the void width. Notably, the initial density distribution of the specimens with initial voids is not uniform. However, the tests were conducted in a constant-volume cell. During this process, slight variations may occur, but the average dry density remains constant. Therefore, the average dry density is used to evaluate the swelling pressure and hydraulic conductivity of the samples.

The swelling pressure and accumulated flow of water for N1, A5, and A6 are shown in Figs. 6 and 7. Compared with N1 and A5, the effect of large voids (S=50%) on the hydromechanical performance of compacted bentonite was investigated. The results indicate that the swelling pressure of both specimens was similar. This trend was consistent with
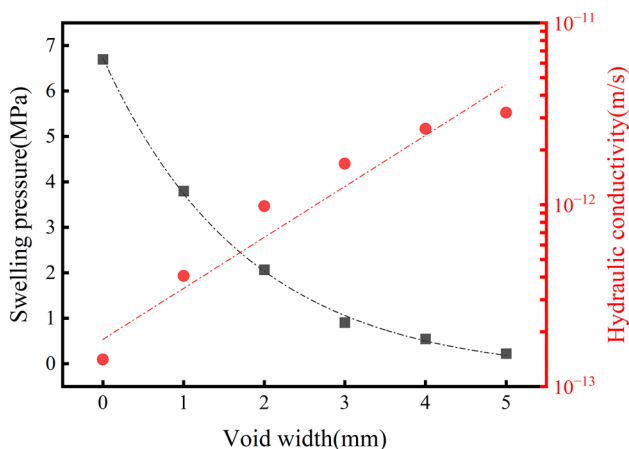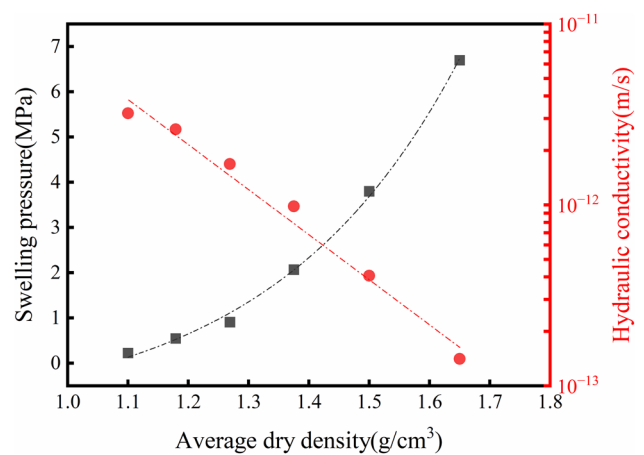

Fig. 5 Relationship of average dry density with swelling pressure and hydraulic conductivity

the findings of Wang et al. (2013), and they thought that the final swelling pressure was independent of the voids. Theoretically, swelling potential of the soil depends solely on the type and content of hydrophilic clay minerals after achieving complete saturation. However, in terms of hydraulic conductivity, the presence of voids leads to overall heterogeneity, and altering the saturation process (Mokni et al. 2016; Millard et al. 2017). When the void volume ratio was 33%, the hydraulic conductivity increased by 10%. Compared with the results of A5 and A6, the swelling pressure was basically the same, but the hydraulic conductivity performance of specimens with SV was better than that of those with CV.

From what has been mentioned above, it can be concluded that the final swelling pressure is not determined independently by the voids or hydration process, but rather by the dry density. However, the presence of voids increases the
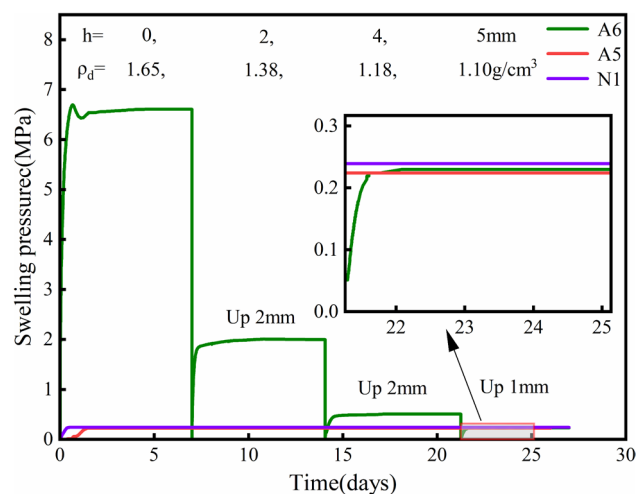

Fig. 4 Relationship of void width with swelling pressure and hydraulic conductivity

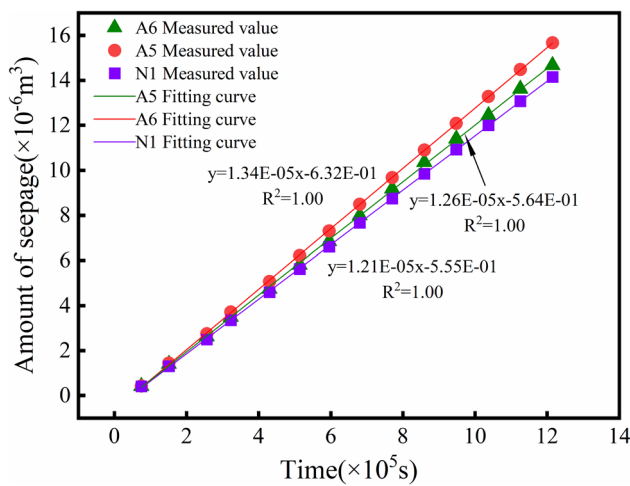**Fig. 6** Comparison of swelling pressure among with NV, SV, and CV

Fig. 7 Comparison of accumulated flow of water among with NV, SV, and CV
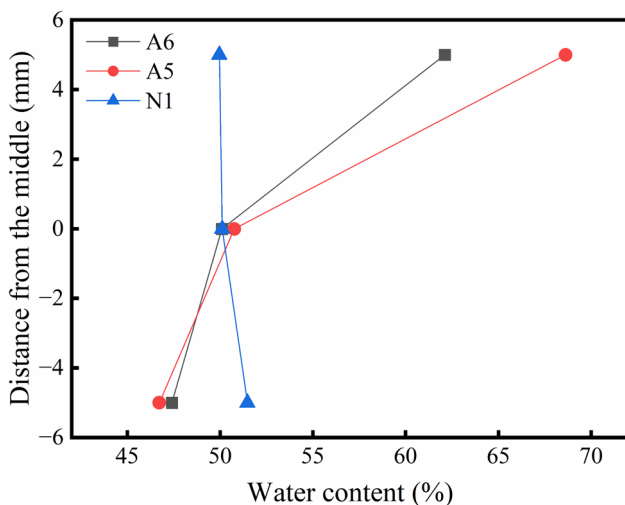

Fig. 8 Distribution of water content

hydraulic conductivity, while the progressive hydration process leads to a slight reduction in the hydraulic conductivity.

Water content analysis

The water content results of the upper (void) layer, middle layer, and lower layer of saturated specimens (N1, A5, and A6) are shown in Fig. 8.

The specimens with pre-set technological voids (A5 and A6) compared to the specimen without voids (N1), there was evident non-uniformity in the water content distribution. The water content in the void part was significantly higher than that in the bottom part, indicating that the structure near the voids was looser and more porous. Saba et al. (2014a, 2014b) explained this finding that bentonite blocks with

construction voids achieved relatively uniform hydration near the void part while the block part taken a much longer time to reach complete uniformity. For N1, because there are no initial voids, the overall structure is relatively uniform, and the water content distribution did not exhibit a clear relationship with the position where specimens were taken.

Comparing the water content of the pre-set technological void specimens (A5 and A6), it was found that the water content in the void part was significantly reduced in SV (A6). However, there was little difference in the water content between the middle and bottom parts of the specimens, indicating that changing the hydration pathway improved the compaction of the void part. It was noteworthy that the water content in the middle part of all three specimens was very close to each other.

MIP analysis

Figure 9 shows the cumulative pore volume distribution curves and pore density distribution curves for the upper and bottom parts of the specimens. A comparison between N1 and A5 revealed significant heterogeneity between the upper void part and the bottom block part in the presence of technological voids. The pore volume at the void part was much larger than that in the bottom part. Conversely, in the absence of void specimens, the upper and bottom parts maintained homogeneity, which was specifically manifested in the similar pore volume and pore size distribution between the upper and bottom parts. These results were consistent with the findings of Jia et al. 0. Notably, whether voids existed or not, there was no significant variation in the pore size distribution of the upper and bottom parts. Additionally, the pore distribution showed a bimodal structure, with the predominant inter-aggregate pores situate in the range of 800–1100 nm. It can be explained that the block preferentially develops in the axial direction with looser spatial constraints during expansion, due to the presence of technological voids. As the position got closer to the voids, there was an increase in the volume of pores within the bentonite aggregate. This observation also confirms the significant difference in water content between the void part and the block part, and the presence of pores can retain more water.

Comparing the results of A5 and A6 tests, it was found that the pore volume of the void part of A6 was smaller than that of A5. While in the bottom parts, it the appeared in opposite. The pore volume difference between the upper and bottom parts of A6 was smaller than that of A5. It indicated that the homogenization degree at the void part of A6 was higher. There were no significant differences in pore size distribution. These results revealed that different pre-set technological void methods have an impact on the hydration development of bentonite. Although the upper and bottom
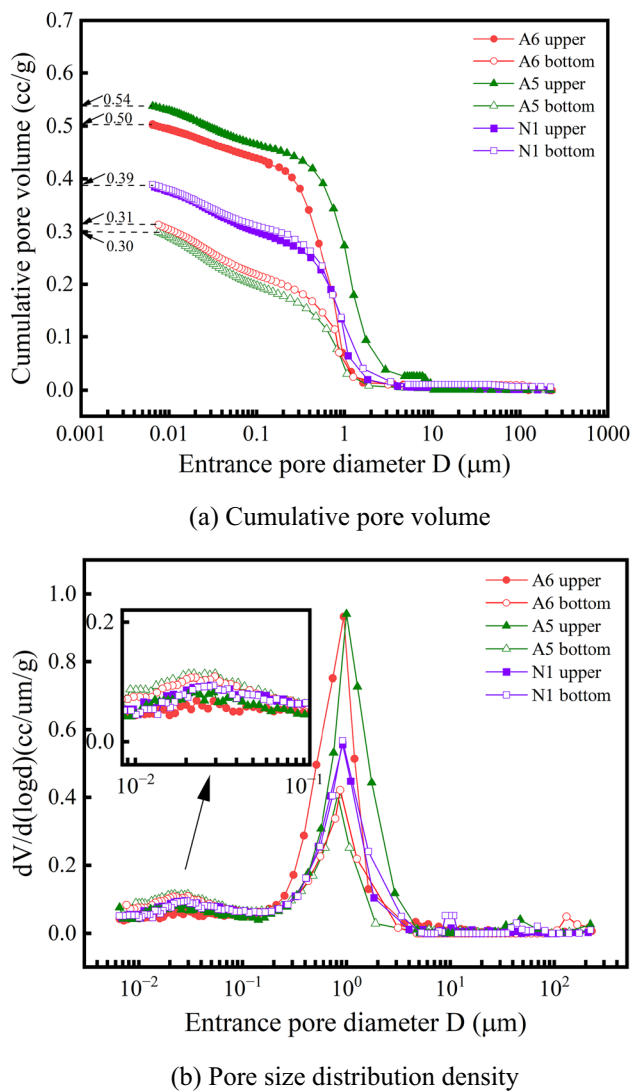
(a) Cumulative pore volume

(b) Pore size distribution density

Fig. 9 Porosity distribution of specimens with NV, SV, and CV

parts of the SV specimen also exhibit significant heterogeneity, overall, it performs better than the CV specimen. This observation was consistent with the results of the saturation and hydraulic conductivity tests. During the hydration process of compacted bentonite blocks, changing the boundary conditions and gradually releasing stress space allow the bentonite to adjust its pore structure gradually, leading to internal particle displacement and rearrangement, and promoting overall homogeneity in its development. Therefore, the hydraulic conductivities under two boundary conditions are different, indicating variations in pore distribution. This highlights the effect of the hydration pathway on the final condition of compacted bentonite blocks. Chen et al. (2017) and Tang et al. (2019) found that different boundary conditions for GMZ bentonite have a significant impact on the swelling behavior of bentonite. Under the same initial conditions, the swelling equilibrium state of bentonite is related

to the hydration pathway and hydration process. Zhang et al. (2016) also found that the development of swelling pressure can be promoted while suppressing expansion strain. It can be observed that the boundary conditions have a significant impact on the hydration process of compacted bentonite blocks and cannot be overlooked.

SEM analysis

SEM analysis is crucial for understanding the effect of voids on the hydro-mechanical behavior of bentonite and the development patterns of blocks under different boundary conditions. Figure 10 presents SEM images of the upper and bottom parts of N1, A5, and A6 specimens, respectively. Compared to the upper part of N1 (Fig. 10a), the upper parts of A5 and A6 (Fig. 10b and c) exhibited distinct characteristics: varying particle sizes, loose particle arrangement, uneven surfaces, abundant pores, and a relatively loose structure. In contrast, the bottom parts of A5, A6, and N1, displayed opposite features: the bottom parts of specimens with technological voids appeared more compact, with smoother surfaces, fewer pores, denser particle arrangement, and less pronounced pore structures. These observed results were consistent with the hydraulic conductivity and pore volume analysis results. For specimens with technological voids, the pore volume notably increases, leading to a significant enhancement in permeability property. Additionally, the SEM results revealed substantial differences between the upper and bottom parts, whereas specimens without voids demonstrate better uniformity between the two parts. In conclusion, the SEM images provide intuitive information about the structural characteristics and pore distribution of bentonite, further confirming the results of hydraulic conductivity and MIP analysis. Microscopic test results suggest that the density distribution of samples with initial voids exhibits heterogeneity after saturation. The measurement of hydraulic conductivity may depend on the dry density of the slice with the highest dry density. In practical tests, it is difficult to determine the exact value and location of the maximum dry density in the samples. Therefore, the average dry density is used as an invariant to describe overall trends and provide a macroscopic evaluation. This approach simplifies the complexity of internal density distribution, allowing us to identify general patterns and behaviors in the data.

In the high-level radioactive waste repository, different boundary conditions of the buffer/backfill material at different locations may result in different swelling behaviors during the saturation process. For the technological voids between bentonite blocks, filling the voids with pellet bentonite will gradually release the stress space of the blocks during the hydration process. This filling process leads to an improvement in the homogeneity of the bentonite block compared to the unfilled. Regarding the different positions
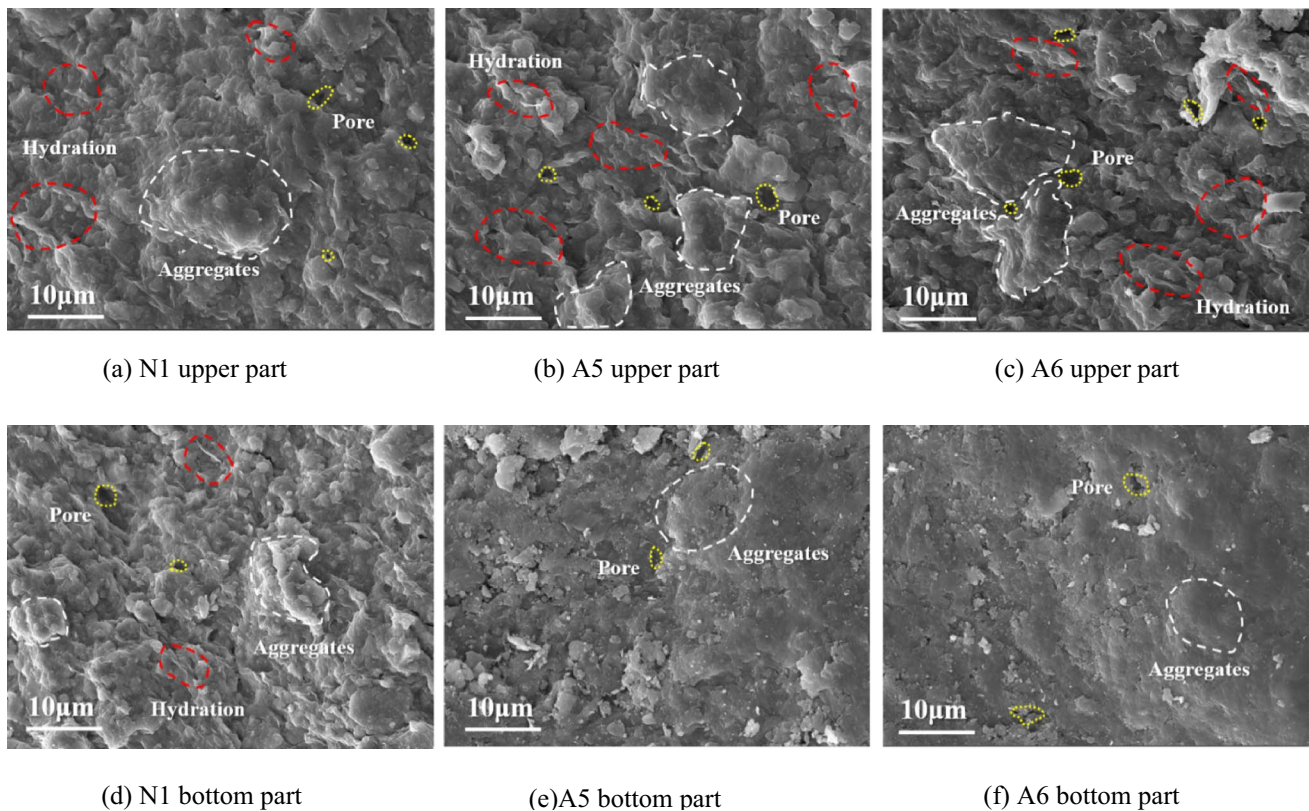
(a) N1 upper part   (b) A5 upper part   (c) A6 upper part

(d) N1 bottom part   (e)A5 bottom part   (f) A6 bottom part

Fig. 10 SEM Images (×5000) of Specimens N1, A5, and A6

of bentonite blocks with technological voids, the outer block undergoes hydration and expansion first to fill the void. Then the inner block undergoes hydration and expansion, under the stress boundary conditions generated by the outer layer blocks. The development pattern of the two is different. This difference poses a new challenge for modeling the buffer layer.

Conclusion

This study investigates the effect of technological voids on the hydro-mechanical behavior of compacted bentonite blocks used in the disposal of high-level radioactive waste. Additionally, the development pattern of blocks under two different boundary conditions was also investigated. Through a comprehensive analysis of swelling pressure, hydraulic conductivity, and microscopic pore tests, the following conclusions are drawn.

1. The swelling pressure of bentonite exhibited an exponential relationship with the width of technological voids, while the hydraulic conductivity coefficient showed a linear relationship with void width. Even with a void volume comprising 33% of the specimen,

the presence of voids does not significantly affect the swelling pressure, which remains solely correlated with the final dry density. However, the existence of technological voids leads to a notable increase in pore volume and a substantial rise in hydraulic conductivity. Moreover, compared to specimens without technological voids, those with voids still exhibited significant differences in pore structure, that was, the pore volume at the void part was larger than that at the bottom part.

2. Under different boundary conditions, the swelling pressure of SV and CV specimens were essentially similar, while the hydraulic conductivity performance of SV specimens slightly outperformed that of CV specimens. Microscopic analysis indicated that SV specimens exhibited higher pore uniformity overall due to the gradual release of expansion space, leading to a reorganization and arrangement of the internal structure of bentonite. The variation in boundary conditions and hydration pathways significantly affects the hydromechanical behavior and pore structure of bentonite. When modeling and designing the buffer layer in high-level radioactive waste repositories, the heterogeneity of bentonite blocks at different positions should be taken into consideration. Further research will concentrate on exploring the hydration behavior of bentonite under dif-

ferent boundary conditions to optimize the design and operation of disposal repositories.

Author contributions Tan: Thesis conception and revision Hu: Test development, data processing, writing Li: Thesis idea and modification Ming: Assist in data processing Wu: Assist in data processing.

Data availability Data will be made available on request.

Declarations

Conflict of interest The authors declare no conflict of interest.

References

Bian X, Cui YJ, Li XZ (2019) Voids effect on the swelling behaviour of compacted bentonite. Géotechnique 69(7):593–605

Birkholzer J, Houseworth J, Tsang C (2012) Geologic disposal of high-level radioactive waste; status, key issues, and trends. Annu Rev Environ Resour 37(1):79–106

Chen B, Chen JQ, Cao YC (2012) Influence of joint on self-sealing behavior of highly compacted bentonite in engineering barrier. Chin J Rock Mech Eng 31(3):618–624

Chen YG, Jia LY, Ye WM, Chen B, Cui YJ (2016) Advances in experimental investigation on hydraulic fracturing behavior of bentonite-based materials used for HLW disposal. Environ Earth Sci 75:787

Chen ZG, Tang CS, Shen Z et al (2017) The geotechnical properties of GMZ buffer/backfill material used in high-level radioactive nuclear waste geological repository: a review. Environ Earth Sci 76:270

Dueck A, Goudarzi R, Börgesson L (2011). Buffer homogenisation, status report. SKB TR-12–02, Svensk Kärnbränslehantering AB

ENRESA (2000) FEBEX project-full scale engineered barriers experiments for a deep geological respiratory for high level radioactive waste in crystalline host rock. In: Final report, Publicación téechnica 4/2002, Empresa Nacional de Residuos Radiactivos SA (ENRESA), Madrid

Feng S, Li T, Zheng W (2024) Experimental study and numerical simulation of coupled thermal-hydro-mechanical behavior of a combined bentonite block-joint sample. Environ Earth Sci 83(10):1–20

García-Siñeriz JL, Villar MV, Rey M et al (2015) Engineered barrier of bentonite pellets and compacted blocks: state after reaching saturation. Eng Geol 192:33–45

Gens A, Vállejan B, Sánchez M et al (2011) Hydromechanical behaviour of a heterogeneous compacted soil: experimental observations and modelling. Géotechnique 61(5):367–386

Gens A, Alcoverro J, Blaheta R et al (2021) HM and THM interactions in bentonite engineered barriers for nuclear waste disposal. Int J Rock Mech Min Sci 137:104572

Gunnarsson D et al (2006) Deep repository–engineered barrier systems. In: Assessment of backfill materials and methods for deposition tunnels, Swedish Nuclear Fuel and Waste Management Co., SKB, R-Series Report R-06–71, SKB, Stockholm

Harrington JF, Daniels KA, Wiseall AC et al (2020) Bentonite homogenisation during the closure of void spaces. Int J Rock Mech Min Sci 136:104535

Jia LY, Chen YG, Ye WM, Cui YJ et al (2019) Effects of a simulated gap on anisotropic swelling pressure of compacted GMZ bentonite. Eng Geol 248:155–163

Komine H (2020) Scale-model test for disposal pit of high-level radioactive waste and theoretical evaluation of self-sealing of bentonite-based buffers. Can Geotech J 57(4):608–615

Liu ZR, Ye WM, Cui YJ et al (2021) Development of swelling pressure for pellet mixture and compacted block of GMZ bentonite. Constr Build Mater 301:124080

Martikainen J, Schatz T (2018) Initial buffer and backfill wetting: pellet-filling component. Eurajoki: Posiva Oy, Eurajoki

Martín PL, Barcala JM, Huertas F et al (2006) Large-scale and long-term coupled thermo-hydro-mechanic experiments with bentonite: the FEBEX mock-up test. J Iber Geol 32(2):259–282

Millard A, Mokni N, Barnichon, et al (2017) Comparative modelling approaches of hydro-mechanical processes in sealing experiments at the Tournemire URL. Environ Earth Sci 76(2):1–19

Mokni N, Barnichon JD, Dick P et al (2016) Effect of technological macro voids on the performance of compacted bentonite/sand seals for deep geological repositories. Int J Rock Mech Min Sci 88:87–97

Narea (2019) Implementation of the full-scale emplacement experiment at mont terri: design, construction and preliminary results. NAGRA Technical Report NTB 15–02:147

Posiva SKB (2017) Safety functions, performance targets and technical design requirements for a KBS-3V repository-conclusions and recommendations from a joint SKB and Posiva working group. In: Posiva SKB Report 01, Posiva Oy, Eurajoki, Finland and Svensk Kärnbränslehantering AB, Stockholm

Saba S, Cui YJ, Tang AM et al (2014a) Investigation of the swelling behaviour of compacted bentonite-sand mixture by mock-up tests. Can Geotech J 51(12):1399–1412

Saba S, Delage P, Lenoir N et al (2014b) Further insight into the microstructure of compacted bentonite-sand mixture. Eng Geol 168(2):141–148

Tan YZ, Xie ZY, Peng F, Qian FH, Ming HJ (2021) Optimal mixing scheme for graphite-bentonite mixtures used as buffer materials in high-level waste repositories. Environ Earth Sci 80:549

Tang CS, Li SJ, Wang DW et al (2019) Experimental simulation of boundary condition effects on bentonite swelling in HLW repositories. Environ Earth Sci 78(5):135.1-135.15

Villar MV, García-Siñeriz JL, Bárcena I et al (2005) State of the bentonite barrier after five years operation of an in situ test simulating a high-level radioactive waste repository. Eng Geol 80(3):175–198

Villar MV, Carbonell B, Martín P et al (2021a) The role of interfaces in the bentonite barrier of a nuclear waste repository on gas transport. Eng Geol 286:106087

Villar MV, Iglesias RJ, Gutiérrez-Álvarez C et al (2021b) Pellets/block bentonite barriers: laboratory study of their evolution upon hydration. Eng Geol 292:106272

Wang Q, Tang AM, Cui YJ et al (2013) The effects of technological voids on the hydro-mechanical behaviour of compacted bentonite–sand mixture. Soils Found 53(2):232–245

Wang Q, Meng YH, Su W et al (2021a) Cracking and sealing behavior of the compacted bentonite upon technological voids filling. Eng Geol 292:106244

Wang Y, Zhang H, Tan Y et al (2021b) Sealing performance of compacted block joints backfilled with bentonite paste or a particle-powder mixture. Soils Found 61(2):496–505

Zeng Z, Cui YJ, Conil N et al (2020) Experimental study on the aeolotropic swelling behaviour of compacted bentonite/claystone mixture with axial/radial technological voids. Eng Geol 278:105846

Zhang F, Ye WM, Chen YG, Chen B et al (2016) Influences of salt solution concentration and vertical stress during saturation on the volume change behavior of compacted GMZ01 bentonite. Eng Geol 207:48–55

Zhang HY, Wang Y, Ma G et al (2018) Stress development in compacted block joints backfilled with bentonite powder in HLW barrier. J Rock Mech Eng 37(09):2200–2208

Zhu CM, Ye WM, Chen YG et al (2013) Influence of salt solutions on the swelling pressure and hydraulic conductivity of compacted GMZ01 bentonite. Eng Geol 166:74–80